DYE SOLUBILITY IN SUPERCRITICAL CARBON DIOXIDE. EFFECT OF HYDROGEN BONDING WITH COSOLVENTS

Poongunran Muthukumaran, Ram B. Gupta[†], Hwan-Do Sung*, Jae-Jin Shim[†]* and Hyo-Kwang Bae*

Department of Chemical Engineering, Auburn University, Auburn, AL 36849-5127, USA
*School of Chemical Engineering and Technology, Yeungnam University, Kyongsan City, Kyongbuk 712-749, Korea

Abstract – The use of supercritical carbon dioxide is emerging as a potential method for achieving pollution-free dyeing. An important factor in supercritical fluid dyeing is the solubility of the dye in supercritical carbon dioxide. Our measurements show that the solubility of C. I. Disperse Red-60 dye in supercritical carbon dioxide is significantly enhanced upon addition of polar cosolvents: ethanol and acetone. The solubility enhancement is attributed to the formation of hydrogen bonds between cosolvent and dye molecules. Observed solubility behavior is correlated using dilute-solution theory with lattice-fluid-hydrogen-bonding model. Needed physical and hydrogen-bonding molecular parameters are estimated using the experimental data.

Key words: Dye Solubility, Supercritical Carbon Dioxide, Hydrogen Bonding, Cosolvent, Solubility Enhancement

INTRODUCTION

With increasing awareness of environmental pollution and strict regulations, the textile industry is continuously looking for environmentally benign processes to replace the existing dyeing methods. In a conventional dyeing process using disperse dyes, a large amounts of water and dispersing agents are used. Dispersing agents are mostly surfactants that increase the dye solubility in water. Treatment of wastewater containing dye and surfactants is a big concern due to its hard-to-destroy characteristics, large volume and color. An alternative to conventional dyeing is the supercritical-fluid dyeing (SFD) process. Supercritical carbon dioxide shows adequate solubility for organic dyes, along with non-toxicity, low viscosity and high diffusivity. In addition, solubility is easily controlled by changing pressure and temperature. Upon release of pressure complete precipitation of dye occurs; hence it is not discarded in the environment, but recovered easily for reuse. Carbon dioxide is the popular supercritical solvent, because of its near-ambient critical temperature, availability and ease of handling. In addition, the SFD gives better dyeing results due to high diffusivity of the dye in the fluid and in the textile, both natural and synthetic polymers. Supercritical CO_2 swells polymer [Shim and Johnston, 1989; Kazarian et al., 1997] and has no surface tension which makes the dye penetration easier than the conventional dyeing process. SFD process is also energy efficient since it does not involve the washing/drying steps that are normally required in conventional aqueous- or solvent-based dyeing.

SFD has been investigated for dyeing polyester [Chang et al., 1996; Saus et al., 1993] and natural fibers [Gerbert et al., 1994; Ozcan et al., 1998]. The solubility of various dyes have been experimentally determined under supercritical conditions
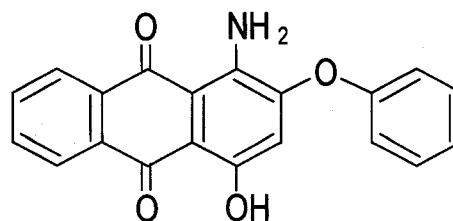

Fig. 1. Molecular structure of C. I. Disperse Red 60 dye.

[Haarhaus et al., 1995; Swidersky et al., 1996; Bae and Her, 1996; Ozcan et al., 1997; Jung and Yoo, 1998], since the solubility plays a key role in the process [Clifford et al., 1996].

Use of cosolvent is known to increase solubility of certain solids [Dobbs et al., 1987; Ting et al., 1993; Ke et al., 1997; Zhong et al., 1997a, b; Foster et al., 1993]. However, the effect of cosolvents on the dye solubility has not been studied yet. Hence, the focus of this work is to study the effect of various cosolvents on the dye solubility. For this study, we have selected 1-amino-4-hydroxy-2-phenoxy anthraquinone, also known as C. I. Disperse Red-60 dye (Fig. 1). Since this dye has hydrogen-bond (H-bond) acceptor and donor sites, polar cosolvents are suitable that can participate in H-bonding. Ethanol and acetone cosolvents are studied here. New experimental data are obtained. Observed solubility behavior is correlated using dilute solution theory with lattice-fluid-hydrogen-bonding model to account for both physical and H-bonding interactions.

EXPERIMENTAL

1. Materials

C. I. Disperse Red-60 dye, not containing dispersing agent or surfactants was obtained from LG Chemical Corp. Ethyl alcohol (99.5 % purity, 1st grade) was obtained from Kanto Chemical Co. Acetone (special grade) was obtained from Yakuri

[†]To whom correspondence should be addressed.
E-mail: gupta@eng.auburn.edu or jjshim@ynucc.yeungnam.ac.kr

P. Muthukumaran et al.

Pure Chemical Co. Carbon dioxide (99% purity) in a siphon-attached cylinder was obtained from Taedong Oxygen Co. These materials were used as received.

APPARATUS AND PROCEDURE

Apparatus and procedure is similar to that described by Sung and Shim [1999] which was used for the dye solubility in pure CO_2. A circulation-type equilibrium apparatus is used which is placed in a constant temperature ($\pm 0.1\,^{\circ}C$) water bath as shown in Fig. 2. A magnetic pump having a small cylinder with a piston inside and a concentric coil outside is used to circulate the fluid between the dye reservoir and the equilibrium cell. The cylinder also serves as an equilibrium cell. Pressure is measured with a transducer (Sensotec TJE) with an indicator (Sensotec GM) calibrated to read the pressure within ± 10 kPa accuracy.

In a typical experiment, a small amount of solid dye is placed in the dye reservoir and both ends are plugged with glass

Fig. 2. Experimental apparatus for measuring dye solubility in supercritical fluid mixture.

wool to prevent the dye powder from being entrained in the fluid during recirculation. Now a known amount of cosolvent (either acetone or ethanol) is injected into the equilibrium cell using a syringe. Then cell is closed and high-pressure connections are made. Using a high-pressure pump (LDC/Milton Roy), liquid carbon dioxide is injected in the system at a desired pressure. Now the mixture in the isolated equilibrium system is circulated with the magnetic pump for 120 minutes until the equilibrium solubility of the dye is attained. Then, the mixture in the equilibrium cell is slowly released to the ethanol-filled trap to collect the dye. Some dye powder precipitates during the depressurization step on the walls of the equilibrium cell, which is recovered by washing with ethanol. Both ethanol solutions are mixed together and analyzed for dye content with a UV/VIS spectrophotometer (Shimadzu UV-160A). The remaining ethanol in the cell is removed by flushing with air, before the next experiment is started.

The dye solubility data are obtained within $\pm 5\%$ error, at varying temperature and pressure. The effect of ethanol cosolvent is shown in Tables 1-2, and the effect of acetone cosolvent is shown in Tables 3-4. These tables also report estimated mixture densities, assuming zero volume of mixing at the given temperature and pressure.

THEORY

Classical thermodynamic models, such as cubic equations of state, generally require critical parameters of the involved components. Unfortunately, these are not available for Red-60 dye. In the case of other equations of state such as lattice-fluid theory [Sanchez and Lacombe, 1976] needed parameters are estimated from pure component properties such as saturated liquid density and vapor pressure at various temperatures. These are also not available for Red-60 dye. Hence an alternate model is
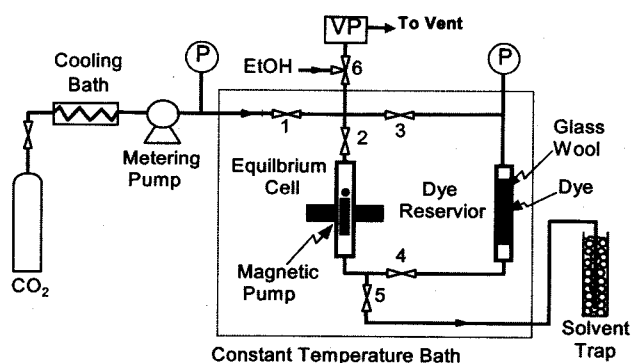
Table 1. Solubility of Red-60 in supercritical CO_2 with ethanol cosolvent at various pressures

Pressure (MPa)	Temperature (°C)	Density (gmol/l)	Ethanol (mol/mol)	Dye solubility (μmol/mol)
14.84	40	18.43	0.043	11.05
17.44	40	19.32	0.043	14.93
23.11	40	20.56	0.043	19.82
30.60	40	21.68	0.043	27.78
13.54	60	12.70	0.043	9.08
20.35	60	17.26	0.043	22.71
22.54	60	18.04	0.043	28.86
29.13	60	19.55	0.043	38.83
33.74	60	20.31	0.043	50.44

Table 2. Solubility of Red-60 in supercritical CO_2 with various amounts of ethanol cosolvent

Pressure (MPa)	Temperature (°C)	Density (gmol/l)	Ethanol (mol/mol)	Dye solubility (μmol/mol)
25.32	40	20.05	0.000	11.44
25.32	40	20.55	0.024	16.58
25.32	40	21.03	0.046	22.84
25.32	40	21.94	0.089	36.66
25.32	60	17.96	0.000	16.00
25.32	60	18.37	0.022	22.88
25.32	60	18.76	0.044	31.3
25.32	60	19.50	0.084	69.49

Table 3. Solubility of Red-60 in supercritical CO_2 with acetone cosolvent at various pressures

Pressure (MPa)	Temperature (°C)	Density (gmol/l)	Acetone (mol/mol)	Dye solubility (μmol/mol)
14.15	60	13.49	0.043	13.46
18.68	60	16.61	0.043	25.11
25.01	60	18.68	0.043	35.47
32.60	60	20.12	0.043	50.85

Table 4. Solubility of Red-60 in supercritical CO_2 with various amounts of acetone cosolvent

Pressure (MPa)	Temperature (°C)	Density (gmol/l)	Acetone (mol/mol)	Dye solubility (μmol/mol)
25.32	60	17.96	0.000	16.00
25.32	60	18.75	0.043	35.47
25.32	60	18.84	0.0478	39.74
25.32	60	19.65	0.0922	80.33

desired for calculations.

Typically, the solubility of solids in supercritical fluids is very small [Ewald et al., 1953; Li et al., 1991; Schmitt and Reid, 1986; Tsekhanskaya et al., 1964]. In the present case dye solubility is of the order of μmol/mol as shown in Tables 1-4. These mixtures can be easily classified as dilute solutions. For dilute solutions, where the solute molecules do not interact with each other, Wang and Tavlarides [1994] have proposed a dilute-solution theory that correlates the phase solubility quite well. We have used the same model as briefly described below.

The chemical potential of a dilute solute (2) in a compressed gas (g) is given by [Wang and Tavlarides, 1994]

$$\mu_2^g = -RT\ln(j_2) + RT(\ln\rho y_2) - \frac{b\rho}{1+c\rho} \quad (1)$$

where, j_2 represents the partition function for all internal degrees of the solute, ρ is the molar density of the mixture, y_2 is the mole fraction of the solute, b and c are temperature-dependent constants for the given solute.

Since the vapor pressure of the solid dye is much smaller than 1 bar, the chemical potential of the dye in the solid phase, μ_2^h, is written as [Prausnitz et al., 1986]

$$\mu_2^h = \mu_{2ref} + RT\ln(P_2^s) + V_2^h(P - P_2^s) \quad (2)$$

where, the reference chemical potential, μ_{2ref}, is related to an arbitrary reference state, P_2^s is the saturation pressure of the pure solute phase at temperature T, and V_2^h is the molar volume of the solid solute.

After equating the chemical potentials of dye in solid phase Eq. (2) to that in the supercritical phase (Eq. (1)), with further analysis [Wang and Tavlarides, 1994], the following equation is obtained

$$\ln\left(\frac{y_2 P}{P_2^s}\right) = \ln\left(\frac{P}{\rho RT}\right) + \frac{b/RT}{1/\rho + c} + \frac{V_2^h(P - P_2^s)}{RT} \quad (3)$$

which is conveniently rewritten as

$$\frac{1}{T\left[\ln\left(\frac{y_2 P}{P_2^s}\right) - \ln\left(\frac{P}{\rho RT}\right) - \frac{V_2^h(P - P_2^s)}{RT}\right]} = \frac{Rc}{b} + \frac{R}{\rho b} \quad (4)$$

So when the left-hand side is plotted versus inverse of density,

the constants are evaluated from slope and intercept in the plot, for given isothermal data set.

COSOLVENT ENHANCEMENT OF SOLUBILITY THROUGH H-BONDING

When polar cosolvents such as ethanol or acetone are added to the system, they H-bond with the dye causing reduction in the chemical potential that, in turn, brings more dye into the supercritical phase. The dye has 3 proton donor sites and 9 proton acceptor sites. Ethanol has 1 proton donor and 1 proton acceptor sites [Gupta et al., 1992]. Acetone has only 2 proton acceptor sites. Hence various kinds of H-bonding are possible. The chemical potential contribution due to the H-bonding is given by lattice-fluid hydrogen-bonding theory [Panayiotou and Sanchez, 1991, Gupta et al., 1992, Gupta et al., 1993] based on statistical distribution of H-bonds between given donor and acceptor sites in close proximity. In the case of ethanol cosolvent, chemical potential of dye due to H-bonding, $\mu_{2,HB-ethanol}$, is given as

$$\frac{\mu_{2,HB-ethanol}}{RT} = r_2\frac{N_{11} + N_{12} + N_{21}}{rN} - 3\ln\left(\frac{3N_2}{3N_2 - N_{21}}\right)$$
$$- 9\ln\left(\frac{9N_2}{9N_2 - N_{21}}\right) \quad (5)$$

Whereas, in the case of acetone, chemical potential of dye due to hydrogen bonding, $\mu_{2,HB-acetone}$, is given as

$$\frac{\mu_{2,HB-acetone}}{RT} = r_2\frac{N_{23}}{rn} - 3\ln\left(\frac{3N_2}{3N_2 - N_{23}}\right) \quad (6)$$

where, 1 represents ethanol, 3 represents acetone, N is the total number of molecules in the mixture, r is the segment length, N_2 is the number of dye molecules, N_{12} is number of ethanol-dye H-bonds, N_{21} is number of dye-ethanol H-bonds, and N_{23} is the number of dye-acetone H-bonds. As the number of H-bonds with dye increases, the chemical potential contribution becomes more negative, due to a large contribution from logarithm term in Eq. (6).

The numbers of H-bonds are estimated by minimizing free energy. For dilute dye concentrations, the number of ethanol-

ethanol H-bonds, N_{11}, is given by

$$\frac{N_{11}}{N} = \frac{1}{2}\left(\frac{2N_1}{N} + A_{11} - \sqrt{A_{11}^2 + 4A_{11}\frac{N_1}{N}}\right) \qquad (7)$$

Number of ethanol-dye H-bonds, N_{12}, is given by

$$\frac{N_{12}}{N} = \frac{1}{2}\left[\frac{N_1}{N} - \frac{N_{11}}{N} + \frac{9N_2}{N} + A_{12}\right.$$

$$\left. -\sqrt{-36\left(\frac{N_1}{N} - \frac{N_{11}}{N}\right)\frac{N_2}{N} + \left(\frac{N_1}{N} - \frac{N_{11}}{N} + \frac{9N_2}{N} + A_{12}\right)^2}\right] \qquad (8)$$

Number of dye-ethanol H-bonds, N_{21}, is given by

$$\frac{N_{21}}{N} = \frac{1}{2}\left[\frac{N_1}{N} - \frac{N_{11}}{N} + \frac{3N_2}{N} + A_{21}\right.$$

$$\left. -\sqrt{-12\left(\frac{N_1}{N} - \frac{N_{11}}{N}\right)\frac{N_2}{N} + \left(\frac{N_1}{N} - \frac{N_{11}}{N} + \frac{3N_2}{N} + A_{21}\right)^2}\right] \qquad (9)$$

Similarly for the acetone case, the number of dye-acetone H-bonds, N_{23}, is given by

$$\frac{N_{23}}{N} = \frac{1}{2}\left[\frac{3N_2}{N} + \frac{2N_3}{N} + A_{23}\right.$$

$$\left. -\sqrt{\left(\frac{3N_2}{N} - \frac{2N_3}{N} + A_{23}\right)^2 - \frac{2N_3}{N}\frac{N_2}{N}}\right] \qquad (10)$$

where, in the above equations the A_{ij} terms are defined as follows.

$$A_{ij} = r\tilde{\rho}\exp\left(\frac{E_{ij}^o + \rho E_{ij}^{\prime o} + PV_{ij}^o - TS_{ij}^o}{RT}\right) \qquad (11)$$

where E_{ij}^0, S_{ij}^0, and V_{ij}^0 are standard energy, entropy, and volume change upon ij H-bond formation, E_{ij}^o is the hydrogen-bond energy correction term due to solvation effect proposed by Gupta et al. [1993], $\tilde{\rho}$ and is the reduced density [Sanchez and Lacombe, 1976].

The chemical potential due to H-bonding is simply added to the physical contribution given by Eq. (1), resulting in a new form of Eq. (3), which is

$$\ln\left(\frac{y_2 P}{P_2^s}\right) = \ln\left(\frac{P}{\rho RT}\right) + \frac{b/RT}{1/\rho + c} + \frac{V_2^h(P - P_2^s)}{RT} - \frac{\mu_{2,HB}}{RT} \qquad (12)$$

In the above equation, $\mu_{2,HB}$ is a negative quantity, hence enhancement in the value of y_2 is observed.

RESULTS AND DISCUSSION

1. Without Cosolvent

Parameters a and b are obtained by fitting Eq. (3) to the dye solubility in CO_2 data [Sung and Shim, 1999] at four temperatures, 40, 60, 90, and 120 °C. A good correlation is obtained as

shown in Fig. 3-4. These temperature-dependent parameters are given as

$$R/b = 0.0016023 - 2.7307 \times 10^{-6}T;$$
$$Rc/b = 0.0003376 - 4.9 \times 10^{-7}T \qquad (13)$$

where T is in degrees Kelvin. The solubility of the dye increases with density of the solvent as expected, and it also increases when temperature is increased due to increased vapor pressure. Fig. 3 represents the extent of non-ideality of the system at 120 °C. It compares the solubility calculated using the ideal-gas law, ideal-gas law with Poynting correction, and dilute solution theory to the experimental data. The dilute solution theory is able to account for the large non-ideality present in the system. Fig. 4 shows experimental and calculated solubility versus density at four different temperatures. The dilute solution theory represents the data well except some deviation for 40 °C at high density. It could be due to the proximity to the critical temperature (31.2 °C). Both theory and data indicate that the solubility can be varied 100 fold by changing the temperature and/or pressure. This ability to control solubility in this wide range will give good control over the rate and color intensity of dyeing.

2. With Cosolvents

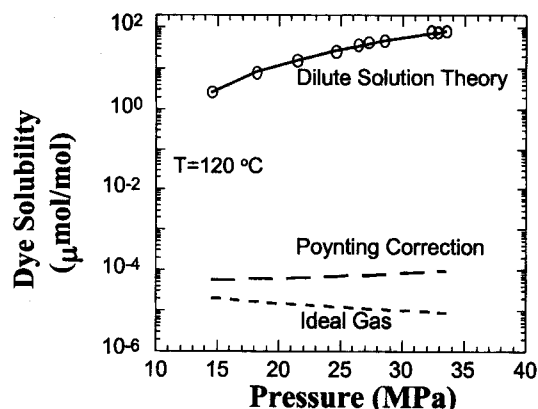Values of ρ^* and r for CO_2 are taken to be 1,510 kg/m³, 6.6,

Fig. 3. Experimental and theoretical dye solubility at 120 °C. High non-ideality is observed due to interaction between supercritical CO_2 and dye molecules.
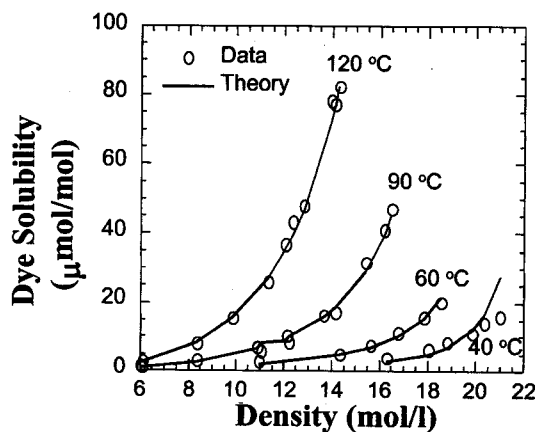
Fig. 4. Experimental [Sung and Shim, 1999] and theoretical dye solubility in CO_2 at 40, 60, 90, and 120 °C.

respectively, r for acetone is taken as 8.4, all from Sanchez and Lacombe [1976]. For ethanol, r is taken as 4.73, and self-association H-bonding parameters are taken as $E_{11}^0 = -25.1$ kJ/mol, $S_{11}^0 = -26.5$ J/mol/K, $V_{11}^0 = -5.6$ cm^3/mol, all from Gupta et al. [1992]. The value of V^0 is considered to be same for all types of H-bonds, for simplicity. H-bonding parameters for dye-ethanol are considered to be the same as ethanol-dye H-bonding, to minimize the number of unknown parameters to be regressed. The r-value for the dye is assumed to be 9.95, the same value as of that for phenanthrene [Sanchez and Lacombe, 1976] which has close resemblance to the dye structure. H-bonding energy and entropy parameters for dye are obtained by fitting Eq. (12) to the dye solubility data with cosolvent (Tables 1-4). Obtained values are: $E_{12}^0 = -31.45$ kJ/mol, $E_{12}^{'0} = 0.394$ kJ./mol^2, $S_{12}^0 = -45.36$ J/mol/K, $E_{23}^0 = -35.47$ kJ/mol, $E_{23}^{'0} = 0.503$ kJ./mol^2, and $S_{23}^0 = -47.49$ J/mol/K.

Fig. 5 compares calculations with experimental data for the effect of ethanol cosolvent on the dye solubility in CO2 at 25.32 MPa and 60 °C. It also shows the calculations if the formation of H-bonds is ignored. Theory can accurately account for the solubility enhancement due to hydrogen bonding. However, theory underestimates the solubility at the highest ethanol loading (8.4 mol%), which may be due to the increase in the critical temperature of the mixture and its reaching close to the system
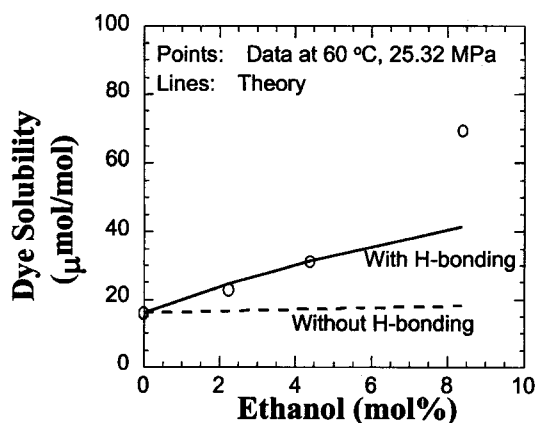

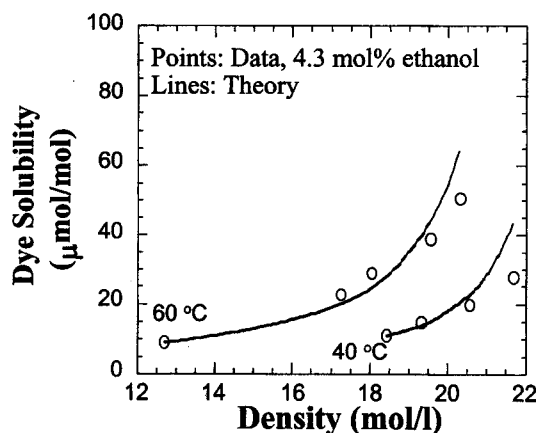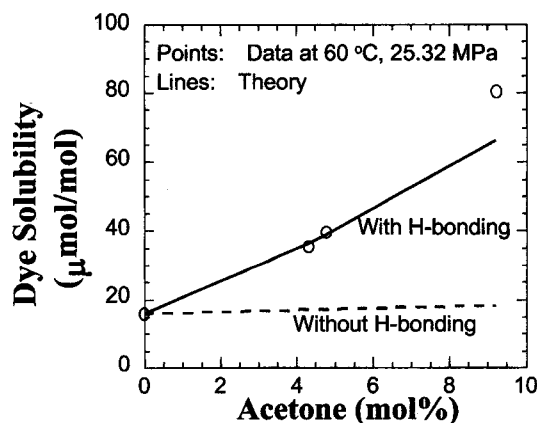Fig. 7. Effect of acetone cosolvent on dye solubility in CO2 at 25.32 MPa, 60 °C.

Fig. 8. Effect of acetone cosolvent on dye solubility in CO2 at 4.3 mol% acetone at varying density.

Fig. 5. Effect of ethanol cosolvent on dye solubility in CO2 at 25.32 MPa, 60 °C.
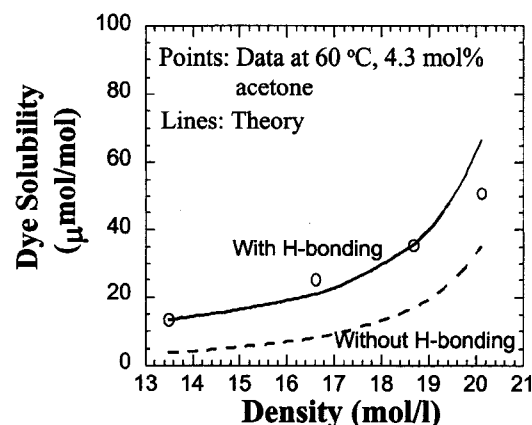

Fig. 6. Effect of cosolvent on dye solubility in CO2 at 4.3 mol% ethanol at varying density.

temperature of 60 °C. Another reason may be that the theory overestimates the ethanol self association at these conditions, because literature H-bonding parameters are used which were obtained from pure ethanol properties, not from ethanol+CO2 mixture properties where CO2 solvation will reduce H-bonding strength. As a result dye-ethanol H-bonds get underestimated, hence the low solubility. Fig. 6 represents the dye solubility versus fluid density at 40 and 60 °C. The theory represents the data reasonably well at this 4.3 mole% ethanol loading.

Fig. 7 shows the effect of acetone cosolvent on the dye solubility at 25.32 MPa and 60 °C, and Fig. 8 shows the effect of fluid density on the dye solubility at a constant acetone mole fraction. Theory is able to properly account for the solubility enhancement due to dye-acetone H-bonding, also.

CONCLUSION

The solubility of C.I. Disperse Red-60 dye in supercritical carbon dioxide at various temperatures, pressures and cosolvent concentrations was obtained using a batch equilibrium apparatus. The dye solubility increased with the addition of polar cosolvents: ethanol and acetone. The dilute solution theory was extended to include hydrogen-bonding interactions, using lattice-fluid-hydrogen-bonding theory. The extended model accurately

correlated the solubility enhancement due to hydrogen bonding which plays an important role in the cosolvent effect.

ACKNOWLEDGMENTS

REFERENCES

Bae, H. K. and Her, B. K., "Solubility of Disperse Dyes in Supercritical Carbon Dioxide," HWAHAK KONGHAK, 34, 379 (1996).

Chang, K. H., Bae, H. K. and Shim, J. J., "Dyeing of PET Textile Fibers and Films in Supercritical Carbon Dioxide," Korean J. Chem. Eng., 13, 310 (1996).

Clifford, A. A. and Bartle, K. D., "Supercritical Fluid Dyeing," Textile and Tech. Int., 113 (1996).

Dobbs, J. M., Wong, J. M., Lahiere, R. J. and Johnston, K. P., "Modification of Supercritical Fluid Phase Behavior Using Polar Co-solvent," Ind. Eng. Chem. Res., 26(1), 56 (1987).

Ewald, A. H., Jepson, W. B. and Bowlinson, J. S., "The Solubility of Solids in Gases," Disc. Farad. Soc., 15, 238 (1953).

Foster, N. R., Singh, H., Yun, S. L. J., Tomasko, D. L. and Macnaughton, S. J., "Polar and Nonpolar Co-solvent Effects on the Solubility of Cholesterol in Supercritical Fluids," Ind. Eng. Chem. Res., 32, 2849 (1993).

Gerbert, B., Saus, W., Knittel, D., Buschmann, H. J. and Schollmeyer, E., "Dyeing Natural Fibers with Disperse Dyes in Supercritical Carbon Dioxide," Textile Res. J., 64(7), 371 (1994).

Gupta, R. B., Combes, J. R. and Johnston, K. P., "Solvent Effect on Hydrogen Bonding in Supercritical Fluids," J. Phys. Chem., 97, 707 (1993).

Gupta, R. B., Panayiotou, C., Sanchez, I. C. and Johnston, K. P., "Theory of Hydrogen Bonding in Supercritical Fluids," AIChE J., 38(8), 1243 (1992).

Haarhaus, U., Swidersky, P. and Schneider, G. M., "High-Pressure Investigations on the Solubility of Dispersion Dyestuffs in Supercritical Gases by VIS/NIR-Spectroscopy. Part 1=1,4-Bis-(octadecylamino)-9,10-anthraquinone and Disperse Orange in CO2 and N2) up to 180 Mpa," J. Supercrit. Fluids, 8, 100 (1995).

Joung, S. N. and Yoo, K. P., "Solubility of Disperse Anthraquinone and Azo Dyes in Supercritical Carbon Dioxide at 313.15 to 393.15 K and from 10 to 25 MPa," J. Chem. Eng. Data, 43, 9 (1998).

Kazarian, S. G., Brantley, N. H., West, B. L., Vincent, M. F. and

Eckert, C. A., "In Situ Spectroscopy of Polymers Subjected to Supercritical CO2: Plasticization and Dye Impregnation," Appl. Spectroscopy, 51(4), 491 (1997).

Ke, J., Jin, S., Han, B., Yan, H. and Shen, D., "Hydrogen Bonding of Some Organic Acid in Supercritical CO2 with Polar Co-solvents," J. Supercrit. Fluids, 11, 53 (1997).

Li, S., Varadarajan, G. S. and Hartland, S., "Solubility of Theobromine and Caffeine in Supercritical Carbon Dioxide: Correlation with Density-Based Models," Fluid Phase Equilib., 68, 263 (1991).

Ozcan, A. S., Clifford, A. A., Bartle, K. D. and Lewis, D. M., "Dyeing of Cotton Fibres with Disperse Dyes in Supercritical Carbon Dioxide," Dyes and Pigments, 36(2), 103 (1998).

Ozcan, S. A., Clifford, A. A. and Bartle, K. D., "Solubility of Disperse Dyes in Supercritical Carbon Dioxide," J. Chem. Eng. Data, 42, 590 (1997).

Panayiotou, C. and Sanchez, I. C., "Hydrogen Bonding in Fluids: An Equation of State Approach," J. Phys. Chem., 95, 10090 (1991).

Prausnitz, J. M., Lichlenthater, R. N. and Azevedo, E. G., "Molecular Thermodynamics of Fluid Phase Equilibria," 2nd ed.; Prentice-Hall Inc., Englewood Cliffs, NJ, Chapter 5 (1986).

Sanchez, I. C. and Lacombe, R. H., "Elementary Molecular Theory of Classical Fluids 2. Statistical Thermodynamics of Fluid Mixtures," J. Phys. Chem., 80, 2352 (1976); also "Elementary Molecular Theory of Classical Fluids. Pure Fluids," ibid., 80, 2568 (1976).

Saus, W., Knittel, D. and Schollmeyer, E., "Farben aus uberkritischem Kohlendioxid-eine Alternative zur HT-Farbung von Polyester," Textile Praxis International, 47, 1052 (1992).

Saus, W., Knittel, D. and Schollmeyer, E., "Dyeing of Textiles in Supercritical Carbon Dioxide," Textile Res. J., 63(3), 135 (1993).

Schmitt, W. J. and Reid, R. C., "The Influence of the Solvent Gas on the Solubility and Selectivity in Supercritical Extraction," In Supercritical Fluid Technology; Penninger, J. M., et al., Eds.; Elsevier; New York, 123 (1985).

Shim, J. J. and Johnston, K. P., "Adjustable Solute Distribution between Polymers and Supercritical Fluids," AIChE J., 35(7), 1097 (1989).

Sung, H. D. and Shim, J. J., "Dye Solubility in Supercritical Carbon Dioxide," submitted to J. Supercrit. Fluids, (1999).

Swidersky, P., Tuma, D. and Schneider, G. M., "High-Pressure Investigations on the Solubility of Dispersion Dyestuffs in Supercritical Gases by VIS-Spectroscopy. Part II 1,4-Bis-(n-alkylamino)-9,10-anthraquinones and Disperse Red 11 in CO2, N2O and CHF3 up to 180 MPa," J. Supercrit. Fluids, 9, 12 (1996).

Ting, S. S. T., Macnaughton, S. J., Tomasko, D. I. and Foster, N. R., "Solubility of Naproxen in Supercritical Carbon Dioxide with and without Co-solvents," Ind. Eng. Chem. Res., 32, 1471 (1993).

Ting, S. S. T., Tomasko, D. L., Macnaughton, S. J. and Foster, N. R., "Chemical-Physical Interpretation of Co-solvent Effects in Supercritical Fluids," Ind. Eng. Chem. Res., 32, 1482 (1993).

Tsekhanskaya, Y. T., Iomtev, M. B. and Mushkina, E. V., "Solu-

bility of Naphthalene in Ethylene and Carbon Dioxide Under Pressure," *Russian J. Phys. Chem.*, **38**(9), 1173 (1964).

Wang, X. and Tavlarides, L. L., "Solubility of Solutes in Compressed Gases: Dilute Solution Theory," *Ind. Eng. Chem. Res.*, **33**, 724 (1994).

Zhong, M., Han, B., Yan, H. and Peng, D. Y., "Effect of Ethanol and n-Octane on the Solubility of Stearic Acid in the Supercritical CO₂," *Fluid Phase Equilib.*, **134**, 175 (1997a).

Zhong, M., Han, B. and Yan, H., "Solubility of Stearic Acid in Supercritical CO₂ with Co-solvents," *J. Supercrit. Fluids*, **10**, 113 (1997b).